



Preparation of Citric Acid-Locust Bean Gum (CA-LBG) for the Disintegrating Agent of Tablet Dosage Forms

Wuryanto Hadinugroho^{1,2} · Suwaldi Martodihardjo² · Achmad Fudholi² · Sugeng Riyanto²

Accepted: 3 October 2021 / Published online: 11 October 2021

© The Author(s), under exclusive licence to Springer Science+Business Media, LLC, part of Springer Nature 2021

Abstract

Purpose Analyze the effect of HCl concentration 0.24 mol as a synthesis catalyst on the viscosity of CA-LBG and determine the effect of the application of CA-LBG as a disintegrating agent on the physical quality of tablets.

Methods Citric acid-locust bean gum (CA-LBG) was synthesized from citric acid (CA) and locust bean gum (LBG) using hydrochloric acid (HCl) and ultraviolet irradiation (UV 254 nm, 100 min). The CA-LBG was analyzed by Fourier transform infrared spectroscopy (FTIR), nuclear magnetic resonance (NMR), scanning electron microscopy (SEM), esterification efficiency, solubility, and viscosity. The tablet formulation used CA-LBG with a concentration variation of 0.5%, 1%, 2%, 4%, 8%, and 12%. Preparation of tablets by direct compression uses a spray dray lactose (SDL) as a filler with a tablet weight of 200 mg.

Results Synthesis conditions using 0.24 mol HCl to produce CA-LBG 9.48 cP. The presence of CA-LBG as a disintegrating agent has variation effects to thickness, break force, tensile strength, and friability according to the concentration used. In the formulation process, increasing the concentration of CA-LBG in the tablet mass decreased the flow rate and increased compressibility.

Conclusion The increase in the concentration of CA-LBG in tablets accelerated the disintegration of tablets without the influence of other tablet parameters. The CA-LBG disintegration activity through repulsion between CA-LBG deformations on the tablet when wetted with disintegration medium. The repulsion force occurs due to the character of CA-LBG which has low solubility and low viscosity.

Keywords CA-LBG · Citric acid · Locust bean gum · Disintegrating agent · Direct compression

Introduction

Natural polymers are a resource that can be used and developed as pharmaceutical excipients. One of the natural polymers in pharmaceutical excipients is locust bean gum (LBG) which functions as the matrix, binder, disintegrating agent, thickening agent, suspending agent, gelling agent, etc. The LBG is a polymer that has the potential to be modified to produce new materials as excipients in tablet formulations [1–4].

Citric acid-locust bean gum (CA-LBG) is a modified polymer synthesized from citric acid (CA) and locust bean gum (LBG). The synthesis was carried out using hydrochloric acid (HCl) as a catalyst and ultraviolet (UV) irradiation as an energy source to form ester bonds. LBG consists of mannose and galactose monomer chains (4:1). [2, 5–9].

The HCl is a strong acid that is effective for creating acidic conditions [10, 11]. Variation is of HCl concentration in the synthesis effect on the character of CA-LBG. The concentration of HCl affects the rate of protonation of the carbonyl group of CA to form a positive C atom. Increasing the concentration of HCl causes an increase in the creation of positive C atoms. This condition increases CA binding to LBG. The characteristics of CA-LBG are influenced by the concentration of CA bound to LBG [6].

The low wavelengths of UV irradiation (200–400 nm) are a source of energy strong enough to form chemical bonds [12–14]. The UV irradiation for a certain duration determines the formation of positive C atoms from the

✉ Wuryanto Hadinugroho
wuryanto.hadinugroho@gmail.com

¹ Department of Pharmaceutical, Faculty of Pharmacy, Widya Mandala Surabaya Catholic University, Kalisari Selatan no. 1 Pakuwon City, Surabaya, Indonesia

² Department of Pharmaceutical, Faculty of Pharmacy, Gadjah Mada University, Sekip Utara, Yogyakarta, Indonesia

carbonyl group in CA with the O atoms (C-6) of mannose and galactose at LBG. The results of previous studies reported that this esterification produced a carbonyl ester group on CA-LBG which was not owned by LBG. In addition, the study reported that CA-LBG has a viscosity of 7–11 cP [6].

The CA-LBG utilization as material synthesis products needs to be studied further. Pharmaceutical formulation is one area where CA-LBG can be used as an alternative to pharmaceutical excipients. Previous studies have reported that CA-LBG has the potential as a disintegrating agent for tablet dosage formulations [6].

The purpose of this study was to analyze the effect of HCl concentration 0.24 mol as a synthesis catalyst on the viscosity of CA-LBG. The aim of the tablet formulation was to determine the effect of the application of CA-LBG as a disintegration agent on the physical quality of tablets. The novelty of this study, the synthesis of CA-LBG uses a concentration of HCl 0.24 mol as the catalyst, and UV irradiation time (100 min) as an energy source that creates the chemical bond. HCl concentrations of 0.18 mol and 0.30 mol were experimental control concentrations to determine the success of the synthesis and characterization of CA-LBG. The CA-LBG experiment as a disintegrating agent was further studied with various concentrations. Sodium starch glycolate (SSG) and croscarmellose sodium (CS) were comparable disintegrating agents to study the disintegration activity of CA-LBG. SSG and CS are tablet disintegrating agents that are often used in tablet formulations because both able to swell in the disintegrating medium in a fast time. The rounded shape with the smooth surface of the SSG and the shape of the root with the corrugated surface of the CS can affect the tablet quality [4, 15]. The experiment was conducted to determine the potential for the disintegration of CA-LBG in tablet formulations as an alternative choice of disintegrating agent to be developed in the future.

Material and Methods

Raw Materials and Chemicals

Materials needed in this study were locust bean gum (Viscogum, Cargill, France), citric acid monohydrate (Merck KgaA, Darmstadt, Germany), hydrochloric acid (Sigma-Aldrich, GmbH, USA), acetone (Cawan Anugerah Chemika, Indonesia), sodium starch glycolate (JRS Pharma, India), croscarmellose sodium (FMC Biopolymer, USA), spray-dried lactose (Foremost Farms, USA), diclofenac sodium (Dwilab Mandiri, Indonesia), sterilized water for injection (Otsuka, Indonesia), and distilled water (Brataco Chemical, Indonesia).

Preparation of CA-LBG

The swollen LBG was placed in a glass bowl (7.10×10^{-6} mol/50 mL concentration at a temperature rate of 55–60 °C) and CA (0.42 mol) was added with different concentrations of HCl (0.18, 0.24, and 0.30 mol). The mixture was stirred for 10 min and irradiated with UV light for 100 min (254 nm, 8-W shortwave CH-4132 Muttenz, Camag, Switzerland). The wet solid was precipitated with acetone and washed with acetone-distilled water (1:1, v/v). The solid CA-LBG was dried at ambient temperature [7].

Chemical characterization was carried out to confirm the success of esterification. The characterization of CA-LBG was performed by using FTIR (Fourier transform infrared) and NMR (nuclear magnetic resonance) spectroscopic techniques. SEM (scanning electron microscope), esterification efficiency, solubility, and viscosity tests were also carried out in order to elucidate the structure.

Fourier Transform Infrared Spectroscopy

The structure and the functional group of CA-LBG were analyzed by Fourier transform infrared spectroscopy (UATR Perkin Elmer Spectrum Version 10.4.3.) in the wavenumber range of 4000–450 cm^{-1} spectra were recorded.

Nuclear Magnetic Resonance

The ^1H and ^{13}C NMR of CA-LBG was analyzed by liquid-state NMR spectroscopy (JEOL RESONANCE ECZ 500R Japan). The CA-LBG (5–15 mg) was stirred for 45 min. The filtrate was placed in the glass tube, and spectra was recorded.

Scanning Electron Microscope

The surface morphology of CA-LBG was analyzed using SEM (JSM-6510LA, JEOL, Japan). The CA-LBG was mounted on a holder, coated by platinum, and observed (distance 10 mm and voltage 10 kV).

Esterification Efficiency

The efficiency of the synthesis was evaluated through the yield percentage of CA-LBG to the total raw material. The evaluation of esterified CA was determined by the degree of esterification. The determination of the degree of esterification follows the experimental equation that has been done previously [6]. Acetone solution and acetone-distilled water to precipitate and wash the acidic CA-LBG mass comes from unreacted HCl and CA. The

concentrations of both were analyzed potentiometrically with NaOH (0.2 N) as the titrant which had been standardized using oxalic acid. The dissolved acid concentration (mEq) was analyzed by means of the titrant volume needed to reach the endpoint of neutralization and was determined according to Eq. 1. The dissolved CA (mEq) is converted (gram) (W_{CA} dissolved), and the reacting CA is determined according to Eq. 2. The carboxylate group weight of the reacting CA (gram) is determined by the mass relative of the carboxylate group compared to the mass relative of CA multiplied by the weight of the CA reacting. The degree of esterification is determined by comparing the CA reacting (gram) and the initial CA (gram) and calculated according to Eq. 3 [6].

Dissolved CA (mEq).

$$\text{dissolved CA [mEq]} = \text{dissolved acid [mEq]} - \text{dissolved HCl [meq]} \quad (1)$$

Weight CA reacting (gram)

$$W_{CA \text{ reacting}} = W_{\text{initial CA}} - W_{\text{dissolved CA}} \quad (2)$$

Degree of esterification

$$\text{Degree of esterification [\%]} = \frac{W_{CA \text{ reacting}} [\text{g}]}{W_{\text{initial CA}} [\text{g}]} \times 100\% \quad (3)$$

Solubility

Solubility was determined by 0.5 g CA-LBG added 50 mL distilled water and allowed to stand for 24 h (W_d). Then, the filtrate was separated from the swollen sample. The filtrate was dried on a water bath at 70 °C and reweighed (W_{ds}) on a microbalance (Mettler Toledo AL204, Switzerland). The solubility of the CA-LBG was analyzed according to Eq. 4:

$$\text{Solubility [\%]} = W_{ds}/W_d \times 100\% \quad (4)$$

where W_{ds} and W_d are soluble weight and initial weight (dry weight, respectively) [16].

Viscosity

The CA-LBG viscosity test is using a viscometer (Brookfield LVDV-I Prime, Middleboro, MA, USA). The CA-LBG (3% w/v) was swelled in 300 mL of warm distilled water and left at ambient temperature. Spindle no. S61 was installed on Brookfield. Viscosity was recorded when Brookfield was rotated at 100 rpm.

Preparation of Tablets

Preparation of tablets begins with weighing the ingredients according to the formula (Table 1). Preparation of tablets by direct compress was prepared by mixing homogeneous SDL and CA-LBG/SSG/CS using a cubic mixer (2 min, 100 rpm) (Erweka). The physical quality of tablet mass was evaluated for flowability and compressibility. The mass of the tablets was compressed with a weight of 200 mg per tablet using a single punch machine (Jenn Chian Machinery, Taiwan). The physical quality of the tablets was evaluated for thickness, weight, break force, tensile strength, friability, and disintegration time.

Flowability

Tablet mass (100 g) was placed in a funnel hole on a flowability tester (Erweka, Germany). When the funnel valve is opened, tablet mass flows. Flow time can be observed on the flowability tester monitor.

Compressibility

Tablet mass was poured into a measuring tube (100 mL, angle $\pm 40^\circ$) whose weight was known. The filled measuring tube is weighed, placed on a tapped density volumeter apparatus (Erweka, Germany), and tapped (500 taps). Weight and volume of tablet mass (before and after tapped) were recorded to determine the bulk density and the tapped density. Tablet mass versus volume before tapped is bulk density. Granule weight/tablet mass versus volume after tapped is the tapped density. The compressibility index is the difference between tapped density and bulk density versus tapped density (Eq. 5) [17].

Table 1 Detail synthesis of CA-LBG using the concentration of HCl and irradiated with UV (254 nm, 100 min). Value physical parameters of CA-LBG: yield, the degree of esterification, carbonyl ester wavelength, solubility, and viscosity

Batch code	LBG 10^{-6} [mol]	CA [mol]	HCl [mol]	Carbonyl ester [cm^{-1}]	Yield [%]	Degree of esterification [%]	Solubility [%]	Viscosity [cP]
A	7.10	0.42	0.18	1739.22	26.62 \pm 0.05	8.27 \pm 0.19	36.63 \pm 1.14	11.20 \pm 0.10
B	7.10	0.42	0.24	1736.39	27.13 \pm 0.09	9.13 \pm 0.13	29.30 \pm 1.16	9.48 \pm 0.06
C	7.10	0.42	0.30	1735.85	27.66 \pm 0.06	9.69 \pm 0.23	22.64 \pm 1.15	7.76 \pm 0.07

$$\text{compressibility index [\%]} = \frac{\text{tapped density} - \text{bulk density}}{\text{tapped density}} \times 100\% \quad (5)$$

Weight and Thickness

Tablet weight and thickness were determined using 20 randomly selected tablets. Each tablet was weighed using an analytical weighing scale (Mettler Toledo, Switzerland), and thickness was accurately measured using a thickness gauge (Mitutoyo 7301, Japan).

Break Force and Tensile Strength

Tablet break force (BF) was determined using 6 randomly selected tablets [18]. The tablet is placed on the break force tester plate (Schleuniger, Netherlands). The metal block moves towards the tablet and presses until the tablet cracks/breaks. The tablet break force value is determined from the start of cracks/breaks, indicated on the monitor.

The strength of the tablet against mechanical stress is determined specifically using the tensile strength parameter according to the shape of the convex tablet. Tensile strength (σt) is calculated following Eq. 6 [19, 20].

$$\sigma t = \frac{10F}{\pi D^2 \left(2.84 \left(\frac{t}{D} \right) - 0.126 \left(\frac{t}{w} \right) + 3.15 \left(\frac{w}{D} \right) + 0.001 \right)} \quad (6)$$

F is the break force, D is the diameter of the tablet, t is the total thickness of the tablet, and w is the thickness of the center of the tablet without convex.

Friability

Tablet friability was determined using a randomly selected number of tablets with a total tablet weight equal to 6500 mg [18]. Each tablet was dust-free, and the total weight of all tablets was determined (W_0). All tablets were put into a drum friability tester (Erweka, Germany) and rotated for 4 min (25 rpm). After being removed from the drum, each tablet was dust-free and weighed again (W_1). The friability of the tablet is the difference in the total weight of the tablet before and after rotated compared to the weight before rotated (Eq. 7).

$$\text{friability[\%]} = \frac{W_0 - W_1}{W_0} \times 100\% \quad (7)$$

Disintegration Time

Tablet disintegration time was determined using 6 tablets randomly selected from 18 previously randomly selected

tablets [18]. Each tablet was inserted into each tube in the chamber disintegration tester apparatus (Erweka Z3, Germany). The chamber is up-down in a distilled water bath (37 °C; 900 mL). The disintegration time was determined from the longest time required for the tube net to be free of tablet fragments.

Dissolution

The experiment was prepared using a tablet mass added with diclofenac sodium as a model active ingredient. Each tablet contains 50 mg of diclofenac sodium to be compressed to a weight of 250 mg [21, 22]. Dissolution using phosphate buffer medium pH 6.8 (900 mL; 37 ± 0.5 °C; 50 rpm) for 60 min using the paddle method (Electrolab TDT-08L, India) [23, 24]. The release of ketoprofen was sampled and observed at 5, 15, 30, 45, and 60 min. Analysis of dissolved diclofenac sodium concentration was done using a UV–VIS is spectrophotometer (Hitachi U-1900, Japan) at a wavelength of 276 nm [25, 26].

Result and Discussion

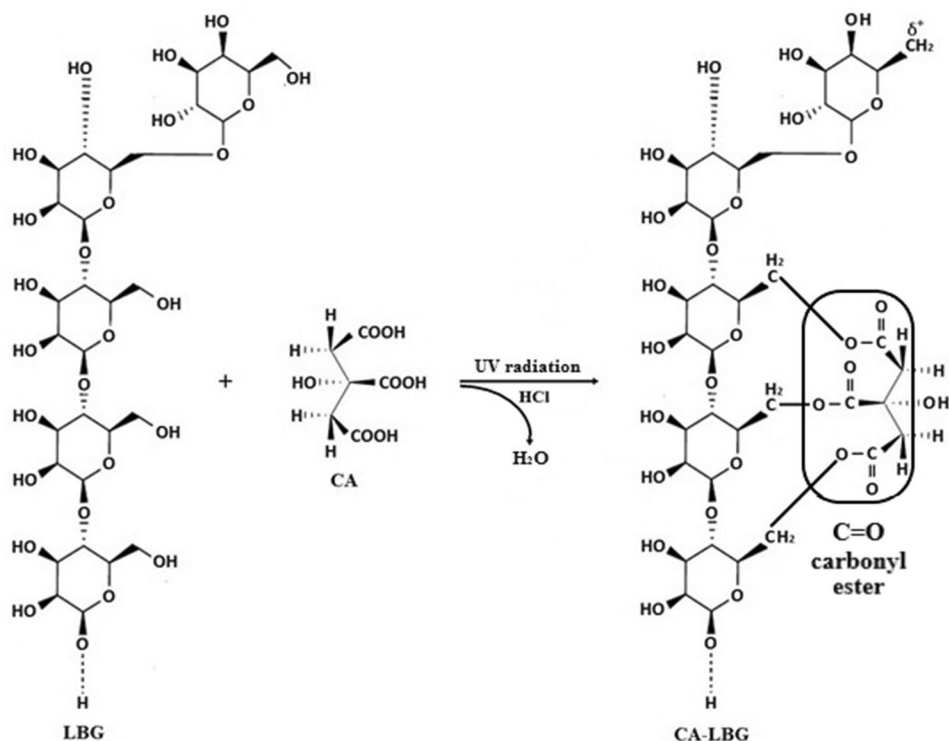
Mechanism of the CA-LBG Synthesis Reaction

In the synthesis of CA-LBG, the acidity of HCl could be induced protonation of O atoms from the carbonyl group of citric acid and created positive C atoms. The hydroxyl (OH) group of C-6 at mannose and galactose atoms reacts with the protonated citric acid carbonyl group to create a tetrahedral cation. Protonated OH ($^+OH_2$) oxygen groups with H_2O loss to form CA-LBG. UV irradiation is the energy source to create bonds between positive C atoms from carboxylic groups and O atoms of C-6 at mannose and galactose [6, 7]. The schematic and details of the synthesis are shown in Fig. 1 and Table 1.

Fourier Transform Infrared Spectroscopy

The results of the CA-LBG and LBG infrared analysis are shown in Fig. 2 and Table 1. The stretching peaks appear at 3268.19 cm^{-1} ; 3291.84 cm^{-1} ; 3304.40 cm^{-1} ; and 3337.34 cm^{-1} are related to the hydroxyl (OH) groups of C atoms at mannose and galactose. Sharp peaks appear at 2920.60 cm^{-1} ; 2923.35 cm^{-1} , 2923.56 cm^{-1} ; and 2923.35 cm^{-1} are related to C–H bonds of CA and LBG. In CA-LBG, the sharp peak comes from C–H symmetrically of CA [27]. The sharp peak of CA-LBG appeared at 1739.22 cm^{-1} , 1736.39 cm^{-1} , and 1735.85 cm^{-1} are related to the carbonyl ester group that was produced from the synthesis reaction. The carbonyl ester group is created by the bond between the positive C atom of the protonated carbonyl

Fig. 1 CA-LBG production mechanism. Synthesis of CA-LBG was carried out by adding 0.42 M CA to 7.10×10^{-6} M LBG which had swollen. The mixture was added with HCl (0.18–0.42 mol) and UV irradiated (100 min)



group in CA and the O atom of C-6 at mannose and galactose in LBG. In a previous study, the OH group appeared around 3300 cm^{-1} . C–H appears around 2900 cm^{-1} , and C=O appears around $1750\text{--}1735 \text{ cm}^{-1}$ [6]. This indicates the success of the synthesis, and CA-LBG was further confirmed by NMR.

Nuclear Magnetic Resonance

The NMR examination was carried out only in one of the experimental conditions (batch B) due to the resulting CA-LBG will be used as a disintegrating agent in the tablet dosage forms. NMR examination of the two other conditions has

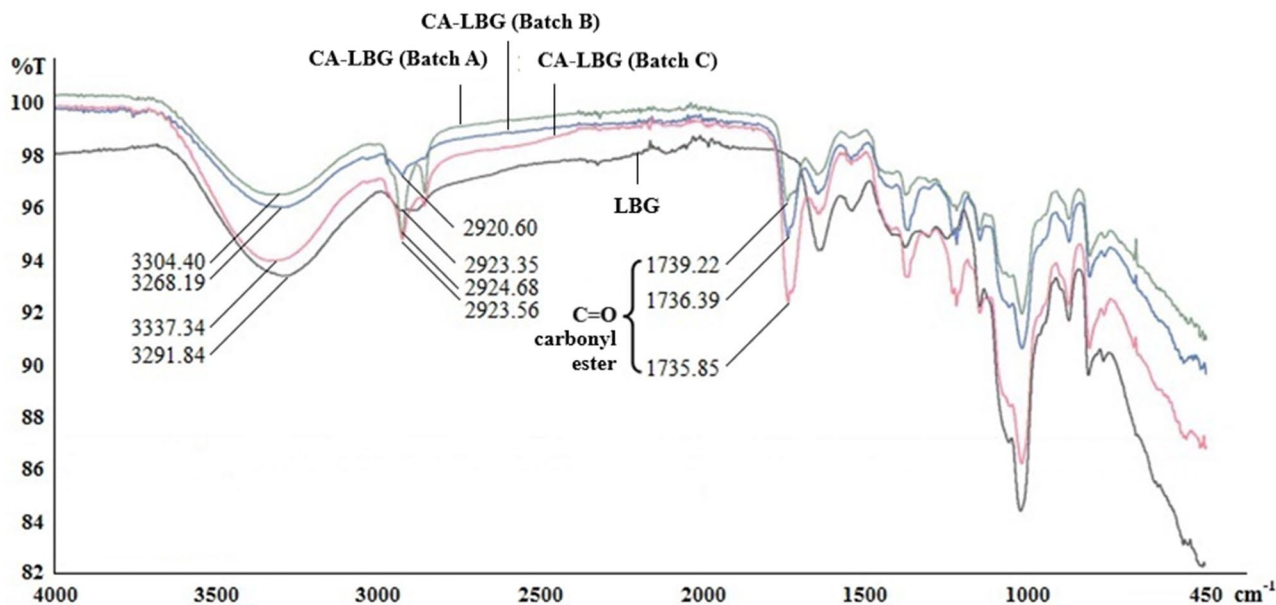


Fig. 2 FTIR spectrum of LBG and CA-LBG. LBG as a comparison is shown in black spectra. CA-LBG was synthesized using a 0.18 mol HCl catalyst (batch A) shown in green spectra. CA-LBG was synthesized using a 0.24 mol HCl catalyst (batch B) shown in blue spec-

tra. CA-LBG was synthesized using 0.30 mol HCl catalyst (batch C) shown in red spectra. The carbonyl ester group (C=O) is a specific group that presents at CA-LBG and is absent at LBG

been confirmed in previous studies [6, 7]. NMR examination using CA-LBG dissolved in deuterium (D_2O) (H_2O).

The results of the CA-LBG NMR analysis are shown in Fig. 3. The 1H NMR spectrum of CA showed two doublet peaks at $\delta=3.088$ ppm and $\delta=3.056$ ppm, $\delta=2.906$ and ppm, and $\delta=2.875$ ppm shows the presence of CA at LBG. The peak is from C-H₂ in CA. The two doublet peaks are protons from symmetric C on CA reacting on LBG. The position of one adjacent proton due to bond rotation and causes the signal to split so that the peak appears splitting. Multiplet peaks at $\delta=4.148$ – 3.587 ppm from mannose and galactose in LBG. Previous studies reported that two doublet peaks of CA around $\delta=2.7$ – 3.0 ppm. Multiple peaks from mannose and galactose appear around $\delta=4.5$ – 3.0 ppm [6, 7].

The peaks of the CA-LBG ^{13}C NMR spectra from the high to low energy field were at $\delta=176.790$ ppm; $\delta=173.459$ ppm; $\delta=173.363$ ppm; $\delta=171.069$ ppm; $\delta=100.192$ ppm; $\delta=100.000$ ppm; $\delta=75.072$ ppm; $\delta=73.325$ ppm; $\delta=71.453$ ppm; 71.338 ppm; $\delta=69.985$ ppm; $\delta=61.260$ ppm, $\delta=61.010$ ppm, and $\delta=60.559$; and $\delta=43.349$. Previous studies reported that the C=O group appeared at $\delta=180$ – 170 ppm, the central C atom appeared at $\delta=80$ – 70 ppm, and C-H and C-H₂ appeared at $\delta=44$ – 43 ppm. [6, 28–30]. The peak absorption of mannose and galactose appears at $\delta=105$ – 60 ppm [6, 31–34]. This shows the success of the synthesis.

Scanning Electron Microscopy

The SEM images of CA-LBG (Batch B) are shown in Fig. 4. In magnification 100 \times , particles of CA-LBG appear in an irregular shape. In magnification 3500 \times , particles CA-LBG have the surface morphology of CA-LBG appear coral-corrugated. Based on previous experiments, LBG has a corrugated morphology and CA creates coral morphology [6]. The LBG particles have a shape coral-corrugated that indicates the available interaction of CA with LBG and shows successful synthesis.

Esterification Efficiency

The yield percentage and degree of esterification of CA-LBG for all batches are shown in Table 1. The high concentration of HCl under synthesis conditions increases yield percentage and degree of esterification due to the high amount of CA bound to LBG. The HCl increases the acidity of the synthesis conditions to protonate the O atom from the carbonyl group and creates a positive C atom, thereby causing CA to bind to LBG. The CA-LBG batch A to batch C shows the higher the degree of esterification in proportion to the increase in the concentration of HCl because the protonation of the O atom from the carbonyl group and the formation of a positive C atom is faster. This condition accelerates creates

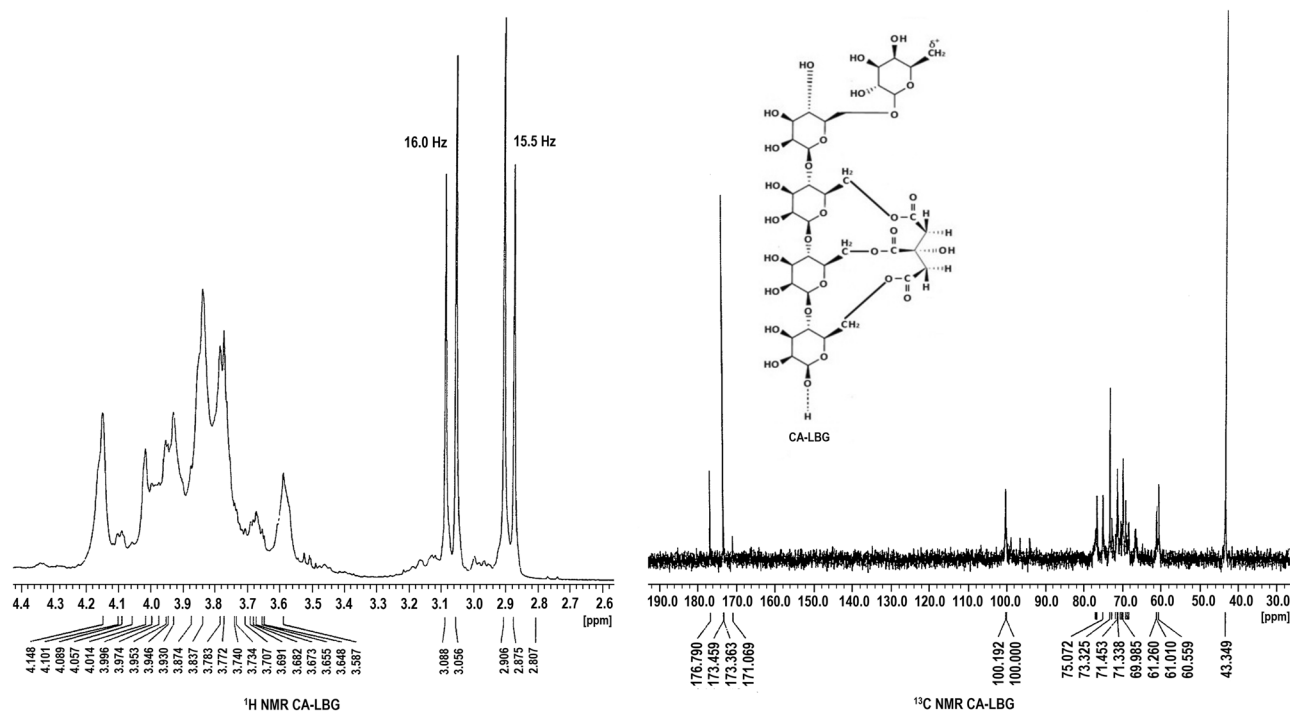


Fig. 3 1H NMR and ^{13}C NMR spectrum of CA-LBG representative (batch B). CA-LBG was synthesized using catalyst 0.24 mol HCl

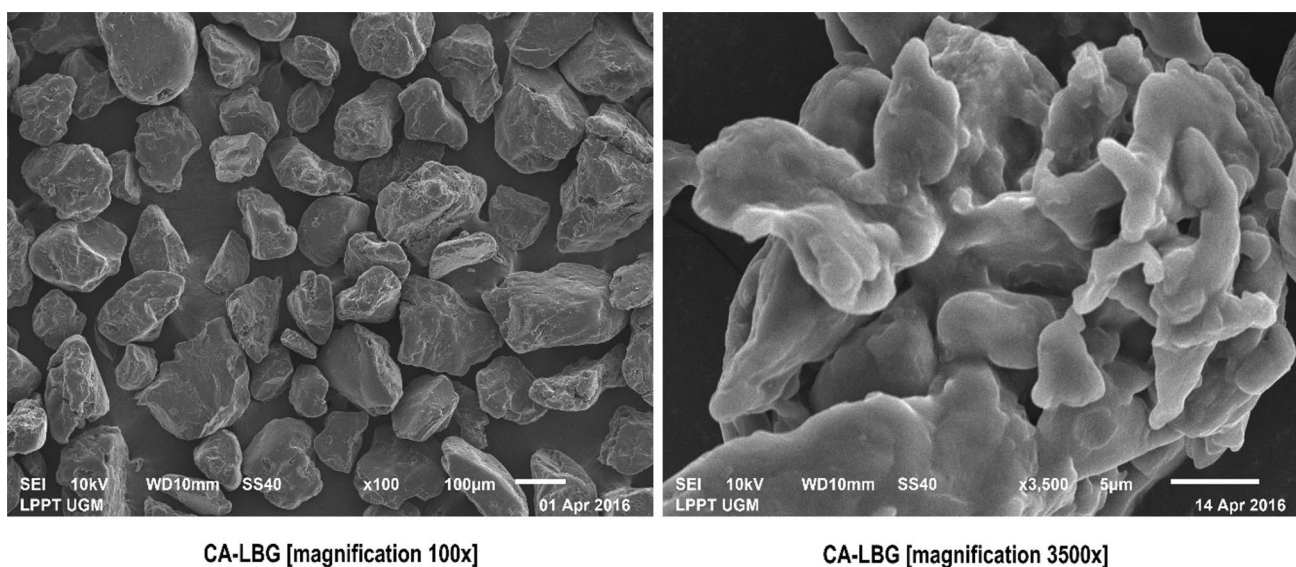


Fig. 4 SEM images of CA-LBG representative, synthesized using catalyst 0.24 mol HCl (batch B)

bonds between positive C atoms from carboxylic groups and O atoms of C-6 at mannose and galactose.

Solubility

The solubility of CA-LBG for each synthesis condition is shown in Table 1. The CA-LBG of batch A to batch B presents the solubility decreasing in proportion to the increasing degree of esterification. The more CA molecules bound to the LBG produce CA-LBG with stable ester bonds. Bonds of positive C atoms from carboxylic groups and O atoms of C-6 at mannose and galactose decrease the ability of CA-LBG to interact with distilled water. In this condition, CA-LBG particles are difficult to wet so inhibit solubility in distilled water.

Viscosity

The viscosity of CA-LBG for each batch is shown in Table 1. LBG has a high viscosity, but the presence of excess CA can reduce the viscosity. The viscosity of CA-LBG from batch A to batch C decreased in proportion to the increasing degree of esterification. The carbonyl ester groups formed from the bonding of positive C atoms from carboxylate groups with O atoms of C-6 in mannose and galactose reduce the ability of CA-LBG to trap distilled water so viscosity decreases.

Flowability

The results of the flowability study on all tablet mass formulas containing CA-LBG showed that an increase in the concentration of CA-LBG increased the flow time of tablet mass (Table 2) because influenced by the irregular shape

of particles and the surface like coral inhibit the flow of mass tablet (Fig. 5). The CL-1 formula has the fastest flow time due to the influence of the spherical shape of the SDL granules to dominate the flowability although CA-LBG is present in the tablet mass [4]. The formula containing SSG and CS showed an increase in concentration cause increased flow time tablet mass. SSG particles are rounded and have a smooth surface and should be able to rate up the flow time, but SSG particles are also hygroscopic, thus inhibiting the flow time of tablet mass [4]. The CS particles are rod-shaped with a corrugated surface, which at high concentrations can inhibit the flow of tablets mass [4]. According to the flow time requirements, all tablet mass formulas containing a variety of disintegrating agents meet the requirements that are 100 g tablet mass that can flow in less than 10 s [35].

The effect of the presence of various disintegrating agents on the tablet mass is shown in Fig. 5, which is a plot between the concentration of the disintegrating agent and the flow rate [g s^{-1}]. In general, the tablet profile containing CA-LBG had the most slope of the flow rate although the CA-LBG concentration was increasing. In addition, the decrease in flow rate of tablet mass with a high concentration of CA-LBG is proportional to the flow rate of tablet mass containing high concentrations of SSG and CS. This case is because the particle surface of CA-LBG like coral can fill each other with a porosity of SDL surface [4]. The sharp decrease in the profile of tablet mass containing CS at low concentrations (CS-1) indicates that the flow rate is more influenced by the spherical shape of the SDL granules so accelerate the flow, while at higher concentrations (CS-2), the root shape and corrugated surfaces of the CS particles begin to inhibit the flow. The flow rate profile of tablet mass containing SSG at low concentrations (SSG-1) is more slope than the

Table 2 Details of tablet formulations using disintegrating agents. Evaluate the physical quality of the tablet mass and the tablet

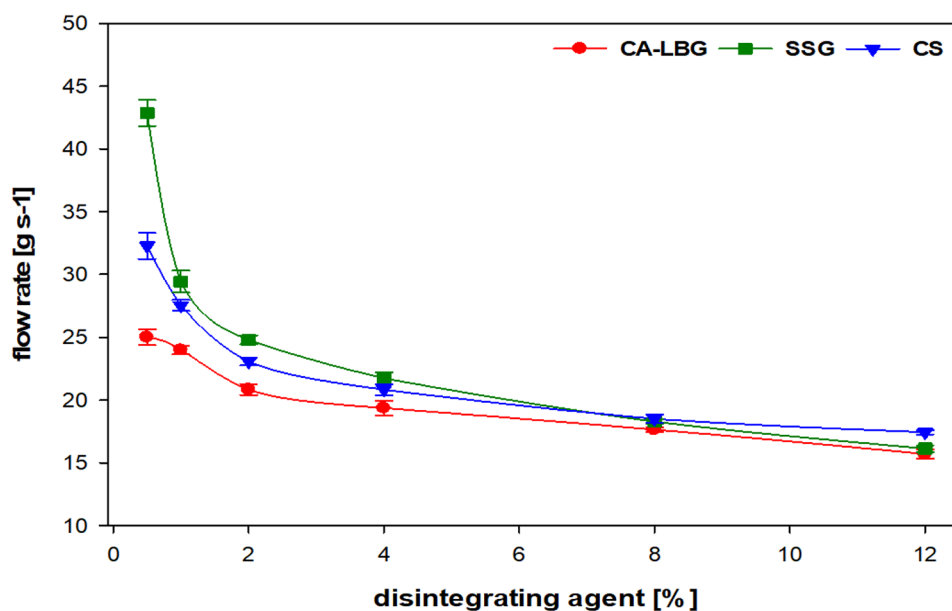
Formula code	Disintegrating agent			Flow time [sec.]	$\rho_{\text{tapped}} - \rho_{\text{bulk}}$ [g.mL ⁻¹]	Actual weight [mg]	Thickness [mm]	Break force [kp]	Friability [%]	Disintegration time [min.]
	CA-LBG	SSG	CS							
	[%]	[%]	[%]							
CL-1	0.5	-	-	4.0±0.10	0.041±0.00	201.0±0.25	4.39±0.01	4.0±0.06	0.76±0.02	9.12±0.34
CL-2	1	-	-	4.2±0.06	0.041±0.00	201.2±0.47	4.38±0.01	4.2±0.10	0.83±0.01	8.54±0.19
CL-3	2	-	-	4.8±0.10	0.044±0.01	201.2±0.12	4.40±0.01	6.4±0.15	0.73±0.02	7.69±0.25
CL-4	4	-	-	5.2±0.15	0.053±0.01	201.1±0.21	4.41±0.01	4.7±0.12	0.66±0.01	6.43±0.14
CL-5	8	-	-	5.7±0.06	0.059±0.01	200.9±0.26	4.38±0.01	4.4±0.10	0.60±0.01	4.47±0.18
CL-6	12	-	-	6.4±0.15	0.061±0.00	201.1±0.36	4.39±0.01	4.4±0.12	0.62±0.01	3.21±0.14
SSG-1	-	0.5	-	2.3±0.06	0.036±0.00	200.8±0.06	4.40±0.01	2.3±0.15	0.85±0.01	3.79±0.25
SSG-2	-	1	-	3.4±0.10	0.042±0.00	201.1±0.44	4.38±0.01	3.0±0.15	0.73±0.02	3.49±0.38
SSG-3	-	2	-	4.0±0.06	0.047±0.01	201.0±0.51	4.35±0.01	6.3±0.12	0.55±0.01	1.73±0.18
SSG-4	-	4	-	4.6±0.10	0.051±0.00	200.7±0.21	4.37±0.01	4.6±0.17	0.60±0.02	0.67±0.09
SSG-5	-	8	-	5.5±0.06	0.057±0.00	201.1±0.32	4.38±0.01	5.0±0.21	0.52±0.02	2.55±0.19
SSG-6	-	12	-	6.2±0.10	0.063±0.00	200.7±0.15	4.38±0.01	4.9±0.12	0.54±0.02	1.90±0.35
CS-1	-	-	0.5	3.1±0.10	0.056±0.00	200.8±0.60	4.43±0.01	4.5±0.12	0.74±0.02	4.37±0.33
CS-2	-	-	1	3.6±0.06	0.052±0.00	200.8±0.35	4.46±0.01	4.7±0.10	0.57±0.02	3.47±0.15
CS-3	-	-	2	4.3±0.06	0.050±0.00	201.0±0.31	4.42±0.01	4.3±0.17	0.69±0.01	2.49±0.12
CS-4	-	-	4	4.8±0.10	0.045±0.00	201.1±0.60	4.40±0.01	6.9±0.12	0.62±0.01	1.60±0.13
CS-5	-	-	8	5.4±0.10	0.038±0.00	201.2±0.35	4.34±0.01	4.5±0.15	0.55±0.01	0.89±0.20
CS-6	-	-	12	5.7±0.06	0.038±0.01	200.9±0.15	4.45±0.01	5.0±0.15	0.56±0.01	0.53±0.30

tablet mass containing CS at the same concentration (CS-1) because the hygroscopicity of SSG particles inhibits the flow of tablet mass. The hygroscopic effect of SSG particles at higher concentrations (SSG-2 to SSG-6) can be overcome by the rounded shape and smooth surface of the SSG particles so that the decrease flow rate is more slope.

Compressibility

The tablet mass density evaluation results on all tablet mass formulas containing CA-LBG or SSG showed that increasing the concentration of the disintegrating agent increased the value of $\rho_{\text{tapped}} - \rho_{\text{bulk}}$ (Table 2), due to the influence of

Fig. 5 The flow rate profile of the mass of the tablet contains a disintegrating agent. The concentration of each disintegrating agent 0.5%, 1%, 2%, 4%, 8%, and 12%



the shape and surface of the disintegrating agent particles. The initial composition of the tablet mass was SDL granules arranged randomly; the porosity between the SDL granules was filled with disintegrating agent particles. The CA-LBG particles which have an irregular shape and a coral-like surface are randomly arranged on the porosity between the SDL granules according to the shape and area of the porosity between the initial particles. The volume decrease during the tapping was caused by the movement of SDL granules and CA-LBG particles. The CA-LBG particle corners fill each other surface porosity between particles and SDL granule surface porosity. In the CL-1 and CL-2 formulas, the porosity of the mass arrangement of tablets was dominated by the effect of the density, and the area of porosity arrangement between SDL granules could accommodate all CA-LBG particles. The volume decrease in the tapping of the formula with the higher CA-LBG concentration causes the porosity between the SDL granules to be wider because the CA-LBG particles surround the SDL granules tightly.

The rounded shape and smooth surface of the SSG particles give a tablet mass arrangement with more regular porosity than the CA-LBG particles. The smooth surface of SSG particles causes movement of SDL granules/SSG particles and decreases in volume during tapping so that the porosity narrows and SSG particles fill the porosity of the SDL granule surface. Formulas containing CS have a different value of $\rho_{\text{tapped}} - \rho_{\text{bulk}}$ from formulas containing other disintegrating agents, namely, the increasing the concentration of CS, the lowering the value of $\rho_{\text{tapped}} - \rho_{\text{bulk}}$. The rod-shaped and corrugated surface of the CS particles is enveloping according to the SDL granule shape in layers and has a narrow porosity. The surface of the CS particles decreases the ability of

the particles to move and the volume decreases on tapping because the surface corrugated of the CS particles will interlock with other CS particles.

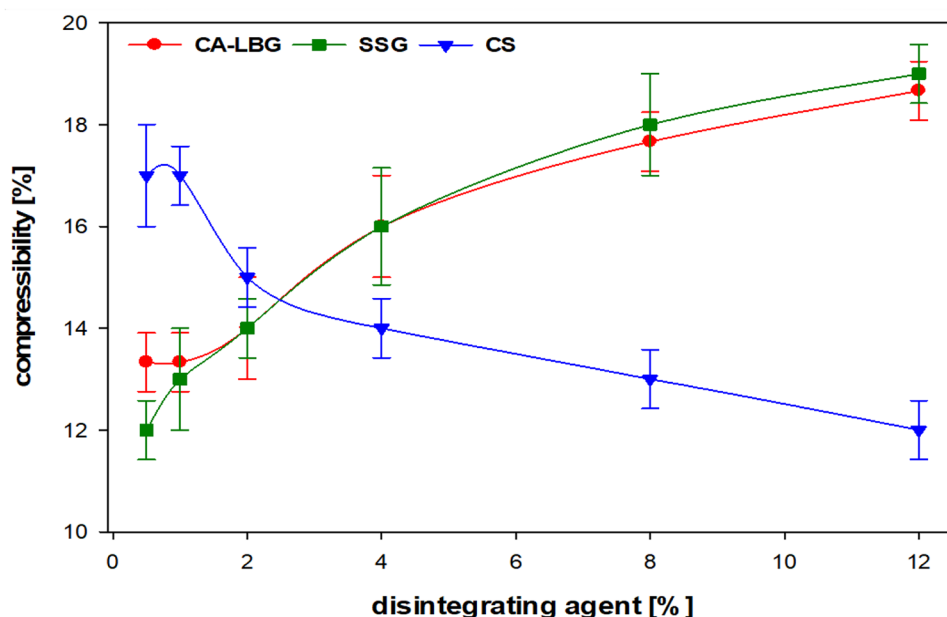
The results of the density evaluation are further confirmed by the compressibility profile shown in Fig. 6, where increasing the concentration of the disintegrating agent increases the mass compressibility of tablets containing CA-LBG/SSG and decreases the mass compressibility of tablets containing CS. The mass compressibility of tablets containing CA-LBG was slightly lower than the mass of tablets containing SSG because the angles of CA-LBG particles fill each other surface porosity between particles and SDL granule surface porosity.

Weight and Thickness

All tablet masses according to each formula were compressed to form tablets weighing about 200 mg (Table 2), which shows that all tablet masses are able to flow freely from the hopper and fill the dead space in the tablet compressing machine. This condition is in accordance with the results of the evaluation of flowability and compressibility.

The variation in tablet thickness from the mass of tablets containing various disintegrating agents is influenced by the arrangement, shape, and surface of the SDL granule or the disintegrating agent particle so that compression is applied produced deformation of the granule/particle, bond interlocking, and narrowing the porosity between deformations. The irregular shape and coral-like surface of the CA-LBG particles provide an opportunity for the particle corners to fill each other with the SDL particle/granule surface porosity

Fig. 6 The compressibility profile of the tablet mass contains a disintegrating agent. The concentration of each disintegrating agent 0.5%, 1%, 2%, 4%, 8%, and 12%



so the tablet mass is compressed to produce a low-porosity tablet. The rounded shape and smooth surface of the SSG particles produce tablets with a regular form of porosity. The root shape and corrugated surface of the CS particles provide an opportunity to interlock between the particles and the corrugated surface so the tablet mass is compressed to produce a low-porosity tablet.

The CL-1 tablet is thicker even though the number of CA-LBG particles is less than the CL-2 tablet because the CA-LBG particles tend to fill the porosity of the SDL granules surface. In the CL-2 tablet, CA-LBG particles fill the surface porosity of SDL granules and porosity between SDL granules. The number of SDL granules of CL-2 tablet mass reduces so that produces a thinner tablet. The CL-3 and CL-4 tablets are thicker than the other CL tablets because the CA-LBG particles surround the SDL granules so that the volume is high and when the tablet mass is compressed into thick tablets. The CL-4 tablet is thicker than the CL-3 tablet due to the increasing number of CA-LBG particles resulting in a wider area surrounding the SDL granules. The number of CA-LBG particles in the CL-5 and CL-6 formula tablets is increasing so the area of the CA-LBG particles surrounding the SDL granules is wider, but the porosity between the CA-LBG particles is narrow so that the mass of the tablets is compressed to produce a thinner tablet. The CL-6 tablet is thicker than the CL-5 tablet because the CA-LBG particle area surrounding the SDL granules is wider.

The SSG-1 tablet is thicker than other SSG tablets because SSG particles fill the porosity of the SDL granules surface so, with the highest number of granules, the tablet mass is compressed to produce thick tablets. Tablet mass of SSG-2 and SSG-3 shows that the number of SSG particles is increasing, and the number of SDL granules is decreasing. The SSG particles in the SSG-2 tablet mass filled the surface porosity of the SDL granules and the dense porosity of the SDL granules. The SSG-3 tablet mass shows the number of SDL granules was reduced so the mass of the tablets was compressed to produce a thinner tablet. The tablet mass of SSG-4 to SSG-6 contains more SSG particles and surrounds the decreasing SDL granules. The SSG-5 tablet is thicker than the SSG-4 tablet because the SSG deformation area surrounding the SDL deformation is wider. The SSG-6 tablet contained more SSG surrounding the SDL deformation with the area is wider. The SSG-6 tablet thickness is similar to SSG-5 because the number of SDL deformation in the tablet mass is reduced.

The thickness of the CS-1 tablet was dominated by the effect filling of CS particles on porosity SDL granules surface, so when compressed, the tablet mass experienced deformation with porosity varying of shapes and areas. The tablet of CS-2 to CS-4 contain more CS particles and fewer SDL granules. The increasing number of CS particles formed the interlocking deformation between the particles

and enveloped the SDL granules so that produce thicker tablets with narrow porosity but in large numbers. The greater the number of CS particles, the wider the enveloping and interlocking area of the CS particles, resulting in a thicker tablet. The thickness of the CS-5 and CS-6 formula tablets was dominated by the increase in the number of CS particles. CS particles are in the CS-5 tablet mass forming long interlocking on surrounding SDL granules. The tablet mass contains limited SDL granules, so it produces thin tablets when compressed. The CS-6 tablet is thicker than the CS-5 tablet because the interlocking area enveloping the SDL granule is wider.

Break Force and Tensile Strength

Evaluation of tablet resistance to mechanical stress is measured by the BF value and shown in Table 2. The resistance of the CL-1 tablet is influenced by the dominance of SDL granules interlocking bonds when compressed to result in deformation with a wide porosity so that the tablets have a low resistance to mechanical stress. The BF value of the CL-2 tablet is higher than CL-1 tablet because the number of CA-LBG particles is more and fills the dense porosity between SDL granules so, when compressed, the interlocking bonds are stronger and the porosity is narrower. The CL-3 tablet shows the highest BF value than other CL tablets because the deformation of CA-LBG particles around the SDL granule when compressed is able to form interlocking bonds with narrow porosity so that the thick tablet is resistant to mechanical stress. In addition, the corners of the CA-LBG particles fill the surface porosity between the CA-LBG particles and the SDL granule surface porosity strengthening the interlocking bond. The CL-4 to CL-6 tablets have a similar mechanism as the CL-3 formula tablets, but the number of CA-LBG particles is increasing, and SDL granules are decreasing so that, when compressed, produce tablets with a lot of narrow porosity and a decrease in tablet resistance to mechanical stress. The tablet of CL-5 and CL-6 shows similar BF values due to the CL-6 tablet, although the interlocking bonds between particles are more dominant with the number of narrow porosity increases.

The SSG particles in the SSG-1 tablet mass fill the surface porosity of the SDL granules, so inducing the granules to be slightly moist and the interlocking bonds between the SDL deformations are weaker. In addition, SDL granules after being compressed produce wide porosity deformation. The resistance of the SSG-2 tablet is higher than the SSG-1 tablet because the narrow porosity between the SDL granules is filled with SSG particles so that the mass of the granules is compressed resulting in a narrower porosity deformation. The SSG-3 tablet shows the strongest resistance than other tablets because SSG particles surround SDL granules when

compressed which are able to form deformation interlocking bonds with narrow and regular porosity, so tablets are resistant to mechanical stress. SSG-4 to SSG-6 tablets have a similar mechanism to SSG-3 tablets, but the number of SSG particles is increasing, and SDL granules are decreasing, so the mass of SSG-5 and SSG 6 when compressed produces tablets with more narrow porosity and decrease in the resistance of the tablet to mechanical stress. In addition, the slightly hygroscopic character of SSG particles decreased the resistance of tablets shown in the SSG-4 tablet because the deformation interlocking bonds of SSG particles around the SDL granules were weak.

The little number of CS particles in the CS-1 tablet tends to fill the porosity of the SDL granules. When compressed, the interlocking bond is dominated by SDL deformation with wide porosity so the resistance of the tablets to mechanical stress is weak. The CS-2 tablet has a similar mechanism to the CS-1 tablet, but the porosity between the SDL granules is filled with CS particles, so it produces a tablet with narrower porosity and is more resistant to mechanical pressure. The CS-3 tablet has a similar mechanism to the CS-2 tablet, but the number of CS particles is more so the CS particles form interlocking between particles and envelop the SDL granules. When compressed, the enveloping CS particles form an interlocking bond deformation with a narrow and large porosity, so the tablet surface resistance is weak. In the CS-4 tablet, the interlocking CS particles to envelope the SDL granules and a wider area so produce tablets with interlocking narrow porosity and strong surface to withstand mechanical stress. The CS-5 and CS-6 tablets have a similar mechanism to the CS-4 tablets, but the number of CS particles is increasing, and the SDL granules are

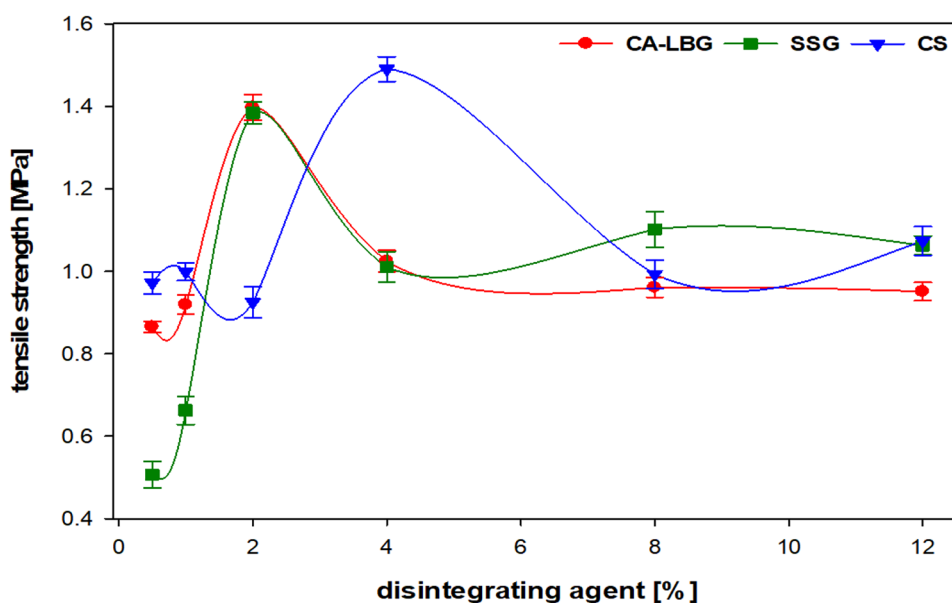
decreasing. In CS-5 tablets, reduced SDL granules have an impact on tablet resistance because SDL granules serve as a foundation to withstand the mechanical stress exerted on the tablet surface. In CS-6 tablets, the foundation of tablet resistance to mechanical stress is controlled more by the interlocking bonds between CS particles after being compressed so that the tablets are stronger than the CS-5 tablet.

The BF value was further confirmed by the tensile strength parameter to determine the comparison between tablets contain disintegrating agent variation according to the concentration in the experiment (Fig. 7). The tensile strength profile of CA-LBG tablets is similar to that of SSG tablets due to the influence of the particle shape of CA-LBG and SSG. The irregular shape and coral surface of the CA-LBG particles produce tablets with strong deformation interlocking bonds. The tensile strength intensity of CA-LBG tablets is similar to that of SSG tablets showing a deformation interlocking bond that can adjust the concentration used in the tablets. In the experiment, the peak of tensile strength of CA-LBG tablets and SSG tablets was at a concentration of 2%, while the peak of tensile strength CS tablets was at a concentration of 4%. This concentration is the optimum condition for forming tablets with the most stable interlocking deformation bonds against mechanical stress.

Friability

Evaluation of tablet resistance to mechanical movement is measured by friability parameters and is shown in Table 2. The friability of the CL-1 tablet is influenced by the low BF value due to the interlocking bond of SDL deformation with wide porosity so that SDL deformation on the tablet surface

Fig. 7 The tensile strength profile of the tablet contains a disintegrating agent. The concentration of each disintegrating agent 0.5%, 1%, 2%, 4%, 8%, and 12%



releases particles when subjected to mechanical movement. In addition, the CA-LBG particles on the tablet surface were also released. The CL-2 tablet is more friable than the CL-1 tablet although the BF value is higher because the number of CA-LBG particles on the surface of the tablet is more, so more particles are released when subject to mechanical movement. The CL-3 to CL-6 tablets showed a tendency to decrease in friability although the BF value was lower because of a strong interlocking bond on the deformation of granules and particles, so reducing the release of tablet surface particles when subjected to mechanical movement. The CL-6 tablet is more friable than the CL-5 tablet because the number of SDL deformation decreases so that the foundation to withstand mechanical movements is reduced.

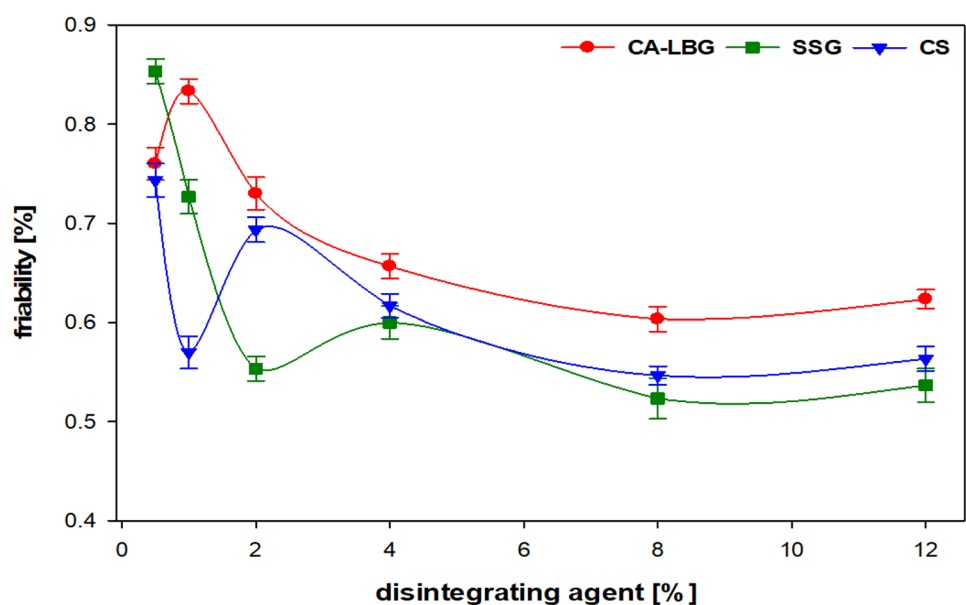
The SSG-1 tablet is the most friable than SSG other tablets because of the low BF value due to SDL deformation interlocking bonds with wide porosity so that the tablet surface releases lactose and SSG particles when subjected to mechanical movement. The decrease in the friability of the SSG-2 and SSG-3 tablets proportional to the higher BF value indicates a strong interlocking bond from the deformation of granules and particles so resistant to mechanical movement. The friability of the SSG-4 to SSG-6 tablets tends to decrease because the strength of the interlocking bonding of SSG deformation is able to withstand mechanical movements. The SSG-6 tablet is more friable than the SSG-5 tablet because the number of SDL deformation is reduced so the foundation to withstand mechanical movements is reduced.

The CS-1 tablet is the most friable than the other CS tablets because the SDL deformation interlocking bond dominates with a wide porosity, so the lactose and CS particles on the surface are released when subject to mechanical

movement. The friability of the CS-2 and CS-3 tablets increased proportionally to the BF values of the two tablet formulas decreased. The more SSG deformation interlocking bonds, the stronger the tablet withstands mechanical movements. The friability of the CS-4 to CS-6 tablets is proportional to the BF value and tends to decrease. The CS deformation on the tablet surface has a strong interlocking bond to withstand mechanical movements. The CS-6 tablet is more friable than the CS-5 tablet because of the reduced deformation of SDL as a foundation to resist mechanical movements.

The comparison of the effect of the presence of the disintegrating agent in each tablet formula to friability according to the concentration in the experiment is shown in Fig. 8. The friability profile of the three CA-LBG tablets is similar but different at the peak of each disintegrating agent (CA-LBG 1%; CS 2%; SSG 4%). These peaks indicate that the tablet surface has bonds weakly of interlocking deformation and is less stable to mechanical movements. The friability value before the peak concentration was also influenced by the release of particles from the SDL deformation, while after the peak concentration was influenced by the quality of the interlocking bond of deformation particles on the tablet surface so resistant to mechanical motion. CA-LBG tablets are more friable than other tablets due to the influence of the coral surface on the particles which tend to be friable when the porosity is not filled with other particles. The high friability profile of CA-LBG tablets appears at low concentrations because the surface porosity of the CA-LBG particles is not filled due to the limited number of CA-LBG particles. In addition, the irregularly shaped CA-LBG particles causing the porosity of tablets were number and wide.

Fig. 8 The friability profile of the tablet contains a disintegrating agent. The concentration of each disintegrating agent 0.5%, 1%, 2%, 4%, 8%, and 12%



Disintegration Time

The evaluation of tablet disintegration rates for all formulas with various disintegrating agents and concentrations is shown in Table 2. The disintegration of tablets containing CA-LBG showed a fast disintegration time proportional to the increasing concentration of CA-LBG. The values of BF and friability do not affect the function of the CA-LBG to disintegrate the tablet. The irregular particle shape and the corrugated surface of the CA-LBG particles resulted in a tablet with porosity for penetration of the disintegrating medium (Fig. 4). The deformation porosity of CA-LBG formed on the tablet is proportional to the CA-LBG concentration in the tablet formula. The porosity of a large number on the tablet cause increases the channel for penetration of the disintegrating medium so that the tablet is disintegrating. The CA-LBG is an ester excipient that has low viscosity and low solubility in water (Table 1). This characteristic causes a repulsive force between deformations of CA-LBG on tablets when wet by disintegration medium. The repulsion force increases in proportion to the CA-LBG concentration in the tablet formula. The repulsive force between the CA-LBG deformations causes the tablets to disintegrate.

Tablets containing SSG showed that SSG concentration, BF value, and friability were influenced the disintegration time. The speed of tablet disintegration time is proportional to the increasing SSG concentration shown in the SSG-1 to SSG-4 tablets. Deformation of SSG in tablets attracts disintegration medium so SSG deformation swells and pushes deformation of other granules and particles to move away from each other so that the tablet is disintegrating. SSG-5 and SSG-6 tablets show the resistance of the tablets to pressure and mechanical movements affect the speed of

disintegration. Increased BF value and low tablet friability caused long tablet disintegration time due to the strong interlocking bond between the deformations of granule or particle, thus inhibiting tablet disintegration.

Tablets containing CS showed an increase in CS concentration causing the disintegration time to rapidly. The resistance of tablets indicated by BF value and friability did not affect the function of CS as a tablet disintegrating agent. Tablets containing CS attracts the disintegrating medium for penetration into the tablet so that the CS deformation swell and push deformation around. The more the CS deformation swell, the faster the tablet integrates.

The comparison of the ability of the disintegrating agent in each tablet formula according to the concentration in the experiment is shown in Fig. 9. The time profile for the disintegration of CA-LBG tablets is similar to that of CS tablets because the two disintegrating agents perform their function not influenced by the quality of other tablets so that the increase in concentration is proportional to the increase in disintegration speed. tablet. In contrast to SSG tablets, the disintegration time is also influenced by the hardness and friability of the tablets, thus inhibiting the disintegration process in tablets with SSG concentrations of 8% and 12%. The disintegration time profile of CA-LBG tablets is longer than CS tablets because low solubility of CA-LBG so that the wetting time of CA-LBG tablets is longer and inhibits integration.

Dissolution

Experiments to study drug release from the dosage form were carried out using tablets of 1%, 2%, and 4% concentrations of each disintegrating agent. The effect of the

Fig. 9 The disintegration time profile of the tablet contains a disintegrating agent. The concentration of each disintegrating agent 0.5%, 1%, 2%, 4%, 8%, and 12%

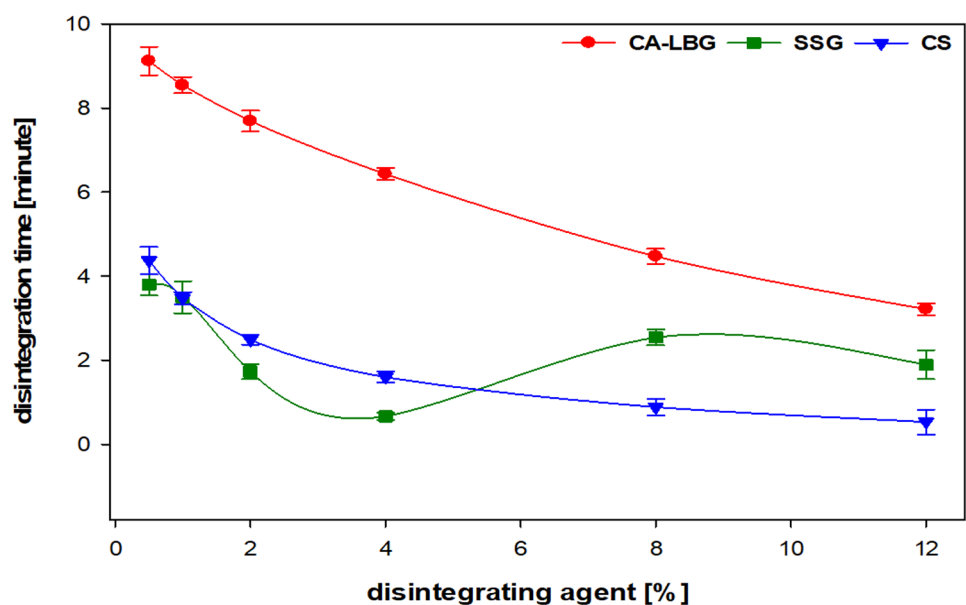


Fig. 10 The dissolution profile of the tablet contains a disintegrating agent. The concentration of each disintegrating agent 2%

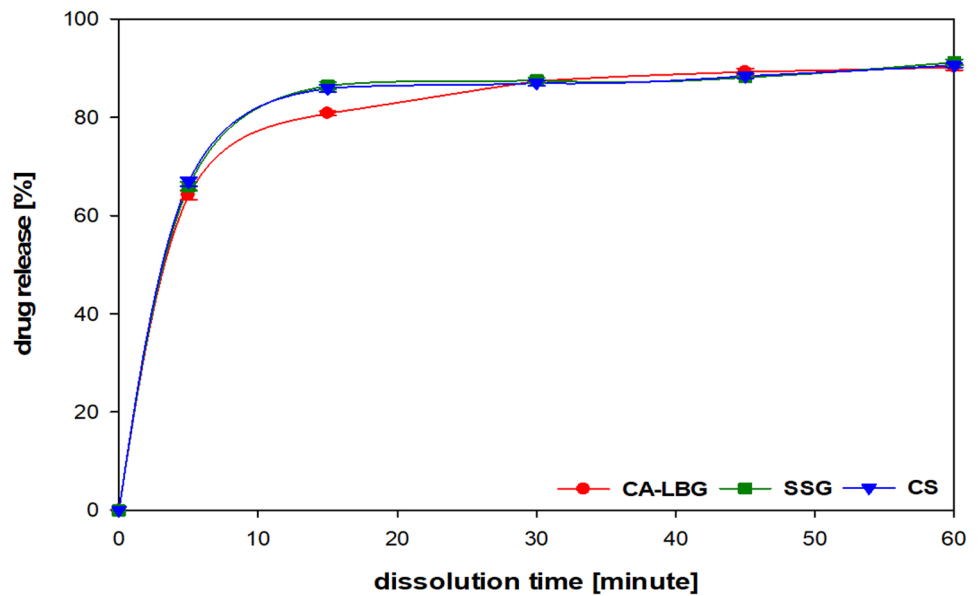
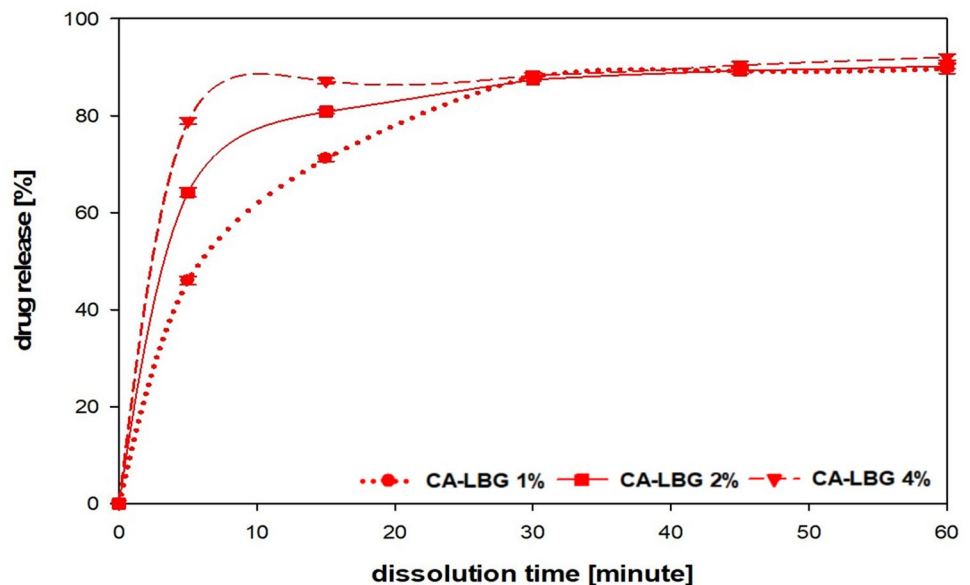


Fig. 11 The dissolution profile of the tablet contains CA-LBG 1%, 2%, and 4%



disintegrating agent on the release of diclofenac sodium from the tablet is presented in Fig. 10. The dissolution profile of the tablets containing CA-LBG showed that the release of diclofenac sodium from the tablets appeared to be different at 5 and 15 min. The higher the concentration of CA-LBG in the formula, the faster the tablet disintegrates and releases more diclofenac sodium. All tablets with each concentration of CA-LBG meet the requirements for releasing diclofenac sodium [36].

A comparison of the release profile of diclofenac sodium from tablets with each of the disintegrating agents was shown in the dissolution profile (Fig. 11). Tablets containing CA-LBG showed a slower release of diclofenac sodium

than tablets containing SSG and CS because of the gradual release at 5 and 15 min. The low solubility of CA-LBG inhibits the wetting of the tablets for disintegration thus inhibiting the solubility of diclofenac sodium in the dissolution medium.

Conclusion

Synthesis conditions using 0.24 mol HCl to produce CA-LBG 9.48 cP. Increasing the concentration of HCl in the synthesis causes a decrease in the viscosity of CA-LBG due to an increase in CA molecules bound to LBG. The presence

of CA-LBG as a disintegrating agent has variation effects to thickness, break force, tensile strength, and friability according to the concentration used. In the formulation process, increasing the concentration of CA-LBG in the tablet mass decreased the flow rate and increased compressibility. The increase in the concentration of CA-LBG in tablets accelerated the disintegration of tablets without the influence of other tablet parameters. The CA-LBG disintegration activity through repulsion between CA-LBG deformations on the tablet is when wetted with disintegration medium. The repulsion force occurs due to the character of CA-LBG which has low solubility and low viscosity.

Supplementary Information The online version contains supplementary material available at <https://doi.org/10.1007/s12247-021-09591-0>.

Acknowledgements The authors thank the research, technology, and higher education department, Indonesia, for support of this work by providing research grants (0299/E3/2016). The author also thanks PT. Makmur Food (Indonesia) for supporting locust bean gum (Viscogum); LPPT Gadjah Mada University (Indonesia) for the SEM, DSC, and NMR instrument support; Faculty of Pharmacy, Gadjah Mada University (Indonesia), for support of pharmaceutical technology facilities; and Faculty of Pharmacy, Widya Mandala Catholic University Surabaya (Indonesia), for pharmaceutical technology facilities and instruments.

Author Contribution Wuryanto Hadinugroho conceived and designed the experiments; performed the experiments; analyzed and interpreted the data; contributed reagents, materials, analysis tools, or data; and wrote the paper.

Suwaldi Martodihardjo, Achmad Fudholi, and Sugeng Riyanto conceived and designed the experiments and analyzed and interpreted the data.

Declarations

Conflict of Interest The authors declare no competing interests.

References

1. Das N, Triparthi N, Basu S, Bose C, Maitra S, Khurana S. Progress in the development of gelling agents for improved culturability of microorganisms. *Front Microbiol.* 2015;6:1–7.
2. Dey P, Maiti S, Sa B. Novel etherified locust bean gum-alginate hydrogels for controlled release of glipizide. *J Biomater Sci Polym Ed.* 2013;24:663–83.
3. Dionísio M, Grenha A. Locust bean gum: exploring its potential for biopharmaceutical applications. *J Pharm Bioallied Sci.* 2012;4:175–85.
4. Sheskey PJ, Cook WG, Cable CG. *Handbook of pharmaceutical excipients 8th.* London-Washington DC: Pharmaceutical Press and American Pharmacists Association; 2017.
5. Chudzikowski RJ. Guar gum and its applications. *J Soc Cosmet Chem.* 1971;22:43–60.
6. Hadinugroho W, Martodihardjo S, Fudholi A, Riyanto S. Esterification of citric acid with locust bean gum. *Heliyon.* Elsevier Ltd; 2019; 5:e02337. <https://doi.org/10.1016/j.heliyon.2019.e02337>.
7. Hadinugroho W, Martodihardjo S, Fudholi A, Riyanto S. Study of a catalyst of citric acid crosslinking on locust bean gum. *J Chem Technol Metall.* 2017;52:1086–91.
8. Samavati V, Razavi SH, Rezaei KA, Aminifar M. Intrinsic viscosity of locust bean gum and sweeteners mixture in dilute solutions. *Electron J Environ Agric Food Chem.* 2007;6:1879–89.
9. Tamaki Y, Teruya T, Tako M. The chemical structure of galactomannan isolated from seeds of *Delonix regia*. *Biosci Biotechnol Biochem.* 2010;74:1110–2.
10. Bhattacharya A, Rawlins JW, Ray P. *Polymer grafting and crosslinking.* Polym. Grafting Crosslink. Canada: A John Wiley & Sons, Inc, Publication; 2008.
11. Colas A. *Cow corning silicones : preparation properties and performance.* Materials. Midland; 2005.
12. Santiago EV, Lopez SHA, Romero AR. Photochemical cross-linking study of polymers containing diacetylene groups in their main chain and azobenzene compounds as pendant groups. *Superf y vacío.* 2006;19:1–7.
13. Tjandraatmadja GF, Burn LS, Jollands MJ. The effects of ultraviolet radiation on polycarbonate glazing. *Proc 8th Int Conf Durab Build Constr Mater Vancouver, Canada.* 1999;30:884–98.
14. Yeh CC, Chen CN, Li YT, Chang CW, Cheng MY, Chang HI. The effect of polymer molecular weight and UV radiation on physical properties and bioactivities of PCL films. *Cell Polym.* 2011;30:261–76.
15. Markl D, Zeitler JA. A review of disintegration mechanisms and measurement techniques. *Pharm Res Pharmaceutical Research.* 2017;34:890–917.
16. Gulrez SKH, Al-Assaf S, Phillips GO. *Hydrogels: methods of preparation, characterisation and applications.* Prog Mol Environ Bioeng - From Anal Model to Technol Appl. 2011.
17. Aulton ME, Taylor K. *Aulton's pharmaceuticals the design and manufacture of medicines.* BMC Public Health. New York: Churchill Livingstone Elsevier; 2017.
18. *The United States Pharmacopeial Convention. Pharmacopeia 41-National Formulary 36.* 41st ed. Rockville: Twinbrook Parkway; 2018.
19. Shang C, Sinka IC, Jayaraman B, Pan J. Break force and tensile strength relationships for curved faced tablets subject to diametrical compression. *Int J Pharm.* Elsevier B.V.; 2013;442:57–64. <https://doi.org/10.1016/j.ijpharm.2012.09.005>.
20. Pitt KG, Newton JM, Richardson R, Stanley P. The material tensile strength of Convex-faced aspirin tablets. *J Pharm Pharmacol.* 1989;41:289–92.
21. Kumar MU, Babu MK. Design and evaluation of fast dissolving tablets containing diclofenac sodium using fenugreek gum as a natural superdisintegrant. *Asian Pac J Trop Biomed.* Hainan Medical University; 2014;4:S329–34. <https://doi.org/10.12980/APJTB.4.2014B672>.
22. Hammami MM, Hussein RF, Alswayeh R, Alvi SN. Eight enteric-coated 50 mg diclofenac sodium tablet formulations marketed in Saudi Arabia: in vitro quality evaluation. *BMC Res Notes BioMed Central.* 2020;13:1–6. <https://doi.org/10.1186/s13104-020-05270-4>.
23. Bertocchi P, Antoniella E, Valvo L, Alimonti S, Memoli A. Diclofenac sodium multisource prolonged release tablets—a comparative study on the dissolution profiles. *J Pharm Biomed Anal.* 2005;37:679–85.
24. Zupančič Božič D, Vrečer F, Kozjek F. Optimization of diclofenac sodium dissolution from sustained release formulations using an artificial neural network. *Eur J Pharm Sci.* 1997;5:163–9.
25. Ghasemi J, Niazi A, Ghobadi S. Simultaneous spectrophotometric determination of benzyl alcohol and diclofenac in pharmaceutical formulations by chemometrics method. *J Chinese Chem Soc.* 2005;52:1049–54.

26. Gouda AA, Kotb El-Sayed MI, Amin AS, El Sheikh R. Spectrophotometric and spectrofluorometric methods for the determination of non-steroidal anti-inflammatory drugs: a review. *Arab J Chem*. 2013;6:145–63. <https://doi.org/10.1016/j.arabjc.2010.12.006>.
27. Coates J. Interpretation of infrared spectra, a practical approach. *Encycl Anal Chem*. 2006;10815–37.
28. Doll KM, Shogren RL, Willett JL, Swift G. Solvent-free polymerization of citric acid and D-sorbitol. *J Polym Sci Part A Polym Chem*. 2006;44:4259–67.
29. Jans AWH, Kinne RKH. ¹³C NMR spectroscopy as a tool to investigate renal metabolism. *Kidney Int*. 1991;39:430–7.
30. Zhang YL, Zhao CX, Liu XD, Li W, Wang JL, Hu ZG. Application of poly(aspartic acid-citric acid) copolymer compound inhibitor as an effective and environmental agent against calcium phosphate in cooling water systems. *J Appl Res Technol*. 2016;14:425–33.
31. Azero EG, Andrade CT. Characterisation of *Prosopis juliflora* seed gum and the effect of its addition to κ-carrageenan systems. *J Braz Chem Soc*. 2006;17:844–50.
32. Bhatia H, Gupta PK, Soni PL, Division C. Extraction, purification and characterization of a galactomannan from *Prosopis juliflora* (Sw.) Dc. Seed. *Int J Sci Environment Technol*. 2013;2:708–24.
33. Gillet S, Aguedo M, Blecker C, Jacquet N, Richel A. Use of ¹³C-NMR in structural elucidation of polysaccharides: case of locust bean gum. *Young Belgium Magn. Reson. Sci. Liege: University of Liege*; 2014.
34. Parvathy KS, Susheelamma NS, Tharanathan RN, Gaonkar AK. A simple non-aqueous method for carboxymethylation of galactomannans. *Carbohydr Polym*. 2005;62:137–41.
35. Szumilo M, Belniak P, Swiader K, Holody E, Poleszak E. Assessment of physical properties of granules with paracetamol and caffeine. *Saudi Pharm J King Saud University*. 2017;25:900–5. <https://doi.org/10.1016/j.jsps.2017.02.009>.
36. Directorate General of Medicine and Food. Indonesian Pharmacopoeia. 4th ed. Jakarta: Ministry of Health Republic of Indonesia; 1995.

Publisher's Note Springer Nature remains neutral with regard to jurisdictional claims in published maps and institutional affiliations.